Using the Suess effect on the stable carbon isotope to distinguish the future from the past in radiocarbon

2016 Environ. Res. Lett. 11 124016

(http://iopscience.iop.org/1748-9326/11/12/124016)

Environmental Research Letters

LETTER

Using the Suess effect on the stable carbon isotope to distinguish the future from the past in radiocarbon

Peter Köhler

Alfred-Wegener-Institut Helmholtz-Zentrum für Polar-und Meeresforschung (AWI), PO Box 12 01 61, D-27515 Bremerhaven, Germany

E-mail: Peter.Koehler@awi.de

Keywords: carbon cycle, future CO_2 emissions, carbon isotopes, radiocarbon dating, Suess effect, modeling, carbon dioxide removal

Supplementary material for this article is available online

OPEN ACCESS

RECEIVED
6 September 2016

REVISED
16 November 2016

ACCEPTED FOR PUBLICATION
18 November 2016

PUBLISHED
7 December 2016

Abstract

The depletion of ^{14}C due to the emission of radiocarbon-free fossil fuels (^{14}C Suess effect) might lead to similar values in future and past radiocarbon signatures potentially introducing ambiguity in dating. I here test if a similar impact on the stable carbon isotope via the ^{13}C Suess effect might help to distinguish between ancient and future carbon sources. To analyze a wide range of possibilities, I add to future emission scenarios carbon dioxide reduction (CDR) mechanisms, which partly enhance the depletion of atmospheric $\Delta^{14}C$ already caused by the ^{14}C Suess effect. The ^{13}C Suess effect leads to unprecedented depletion in $\delta^{13}C$ shifting the carbon cycle to a phase space in $\Delta^{14}C$–$\delta^{13}C$, in which the system has not been during the last 50 000 years and therefore the similarity in past and future $\Delta^{14}C$ (the ambiguity in ^{14}C dating) induced by fossil fuels can in most cases be overcome by analyzing ^{13}C. Only for slow changing reservoirs (e.g. deep Indo-Pacific Ocean) or when CDR scenarios are dominated by bioenergy with capture and storage the effect of anthropogenic activities on ^{13}C does not unequivocally identify between past and future carbon cycle changes.

1. Introduction

One of the side effects of anthropogenic CO_2 emissions is the so-called (^{14}C) Suess effect (Suess 1955), the depletion of the radiocarbon isotopic signature of atmospheric CO_2 due to the injection of large amounts of ^{14}C-free fossil fuels (Stuiver and Quay 1981). It has been shown with models (Caldeira *et al* 1998, Graven 2015) that by the end of the 21st century for most emission scenarios atmospheric $\Delta^{14}C$ might be smaller than $\Delta^{14}C$ in surface and intermediate oceanic water masses. This would reverse the past and present day atmosphere-to-ocean gradient in $\Delta^{14}C$ and complicate conventional radiocarbon dating. For example, from the year 2050 onward fresh organic material might have the same $^{14}C/^{12}C$ ratio as samples from 1050 CE and earlier, making both past and future samples indistinguishable if analyzed by radiocarbon dating alone (Graven 2015).

Not yet mentioned in this previous analysis (Graven 2015) is the fact that ^{13}C is also affected by anthropogenic CO_2 emissions, since most of the released carbon has its origin in organic material, in which ^{13}C is depleted with respect to ^{12}C due to isotopic fractionation during photosynthesis (Lloyd and Farquhar 1994). Charles Keeling named this the *^{13}C Suess effect* (Keeling 1979), which has since then been widely observed in carbon reservoirs, e.g. in the atmosphere (Rubino *et al* 2013) and the surface ocean (Gruber *et al* 1999, Swart *et al* 2010, Schmittner *et al* 2013).

To project how emissions and therefore the Suess effects might develop in the future the international commitments to act against ongoing anthropogenic emissions need to be considered. Climate negotiations during the 21st Conference of Parties of United Nations Framework Convention on Climate Change in December 2015 in Paris have strengthened the political will to keep global warming caused by mankind under some agreed-upon thresholds (Iyer *et al* 2015), whose details are still a matter of debate (Knutti *et al* 2016). To meet such global warming thresholds, and to operate against a likely CO_2 overshoot, not only a reduction in fossil fuel emissions (Rogelj *et al* 2013),

but also some active CO_2 removal from the atmosphere might be necessary (Smith *et al* 2016b) in order to achieve net zero emissions on the long-term (Rogelj *et al* 2015). Furthermore, once net zero emissions are achieved the rebound effect (Cao and Caldeira 2010), the outgassing of anthropogenic CO_2 previously taken up by the ocean, might also urge mankind to implement negative CO_2 emissions or carbon dioxide reduction (CDR) mechanisms in order to keep atmospheric CO_2 at the desired concentration.

Model-based analysis of various CDR approaches are the subject of ongoing research. Within the most recent assessment of CDR (Smith *et al* 2016b) various different approaches have been compared with respect to their requirements in terms of energy, land, nutrient and water usages, their impacts on albedo and their costs. One of the CDR approaches analyzed in that study (bioenergy (BE) with carbon capture and storage (CCS), combined to BECCS) has already been implemented in some of the Representative Concentration Pathway (RCP) emission scenarios used for the most recent IPCC report (Meinshausen *et al* 2011, van Vuuren *et al* 2011). The magnitude of BECCS was up to 3.1, 1.2 and 0.2 PgC yr^{-1} in RCP2.6, RCP4.5 and RCP6.0, respectively, compensating for some of the fossil fuel emissions and leading in RCP2.6 to negative CO_2 emissions at the end of this century (figure 1(A) inlet).

I will here have a look at potential changes in the carbon isotopes in the future and analyze how the ^{13}C Suess effect might help to solve the proposed future radiocarbon dating conundrum caused by the ^{14}C Suess effect. For this aim I will extend the analysis of the emission scenarios to the year 2500 using the well tested carbon cycle box model BICYCLE (Köhler *et al* 2005), which is described in detail in the supplementary material. The extensions of the RCP emissions scenarios beyond the year 2100 were labeled the Extended Concentration Pathways (ECPs) (Meinshausen *et al* 2011). However, for reasons of simplicity I here address the emission scenarios as 'RCP', no matter if it concerns changes until or after the year 2100. I will also incorporate how the carbon cycle might be further affected by some CDR methods discussed nowadays to cover an as wide as possible range of potential changes in ^{13}C and ^{14}C. Finally, I set the simulated future dynamics in the carbon isotopes into perspective of what is known from paleo data (and modeling) covering the last 50 000 years.

2. Simulation scenarios

I use the historical anthropogenic carbon release (1765–2005) from both fossil fuel emissions (including cement production) and land use changes

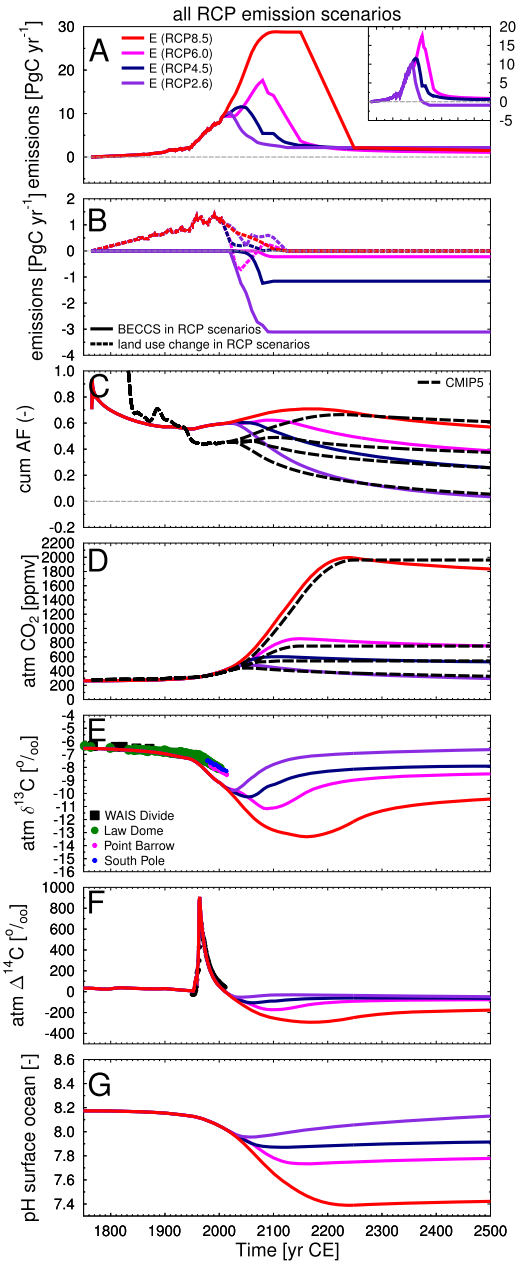

Figure 1. Future carbon cycle simulation results until year 2500 for all four emission scenarios (RCP2.6, RCP4.5, RCP6.0, RCP8.5) (Meinshausen *et al* 2011). (A) Total anthropogenic emissions rates *E* (sum of fossil fuel and land use change emissions). Net emissions (E–BECCS in PgC yr^{-1}) for RCP2.6, RCP4.5, RCP6.0 are shown in the small inlet. (B) Contributions of land use change emissions to and prescribed CDR via BECCS already contained in the respective RCP scenarios. (C) Cumulative airborne fraction (AF): $\Delta A/\sum E$ with ΔA change in atmospheric C content and $\sum E$ the cumulative sum of emissions. (D) Simulated atmospheric CO_2, black broken lines are the past reconstruction of CO_2 (instrumental at Mauna Loa) (Keeling and Whorf 2005) and Law Dome ice core (Rubino *et al* 2013) or the mean of projected future concentrations of emission driven simulations within CMIP5 for the different RCP scenarios (Meinshausen *et al* 2011); (E) Simulated atmospheric $\delta^{13}C$ and reconstructions (instrumental: Point Barrow, South Pole, Keeling *et al* 2001, ice cores: Law Dome and WAIS Divide, Rubino *et al* 2013, Bauska *et al* 2015); (F) Simulated atmospheric $\Delta^{14}C$ including in black the reconstructed radiocarbon bomb peak (Hua *et al* 2013); (G) Simulated mean pH of the surface ocean.

(figure S1A) as contained in the extended version of the RCP emission scenarios (Moss *et al* 2010, Meinshausen *et al* 2011), which proposed carbon emissions from 2006 onward until the year 2500 (figure 1(A)). The historical emission fluxes contained in the RCP scenarios (Meinshausen *et al* 2011) are slightly smaller in the 2nd half of the 20th century than in those previously published (Houghton 2003) due to some downward correction of the land use emission fluxes. Assumptions then have to be made on the isotopic signature of the emissions (figure S1B): the $\delta^{13}C$ signature of fossil emissions is taken from reconstructions between 1765 and 2011 and kept constant at its 2011 value thereafter (Andres *et al* 2000, 2015), while that from land use change is internally calculated from the atmospheric $\delta^{13}C$ value using the isotopic fractionation during C_3 photosynthesis by −19‰. Similarly, the ^{14}C signature from land use emissions is derived using twice the named isotopic fractionation for $\delta^{13}C$, while fossil fuels are assumed to contain no ^{14}C. I only consider CO_2 emissions, all other anthropogenic emissions contained in the RCP scenarios are neglected.

The ^{14}C production rate is prescribed before 1950 CE (Roth and Joos 2013) varying around a mean production rate of 440 mol per year, kept constant thereafter with individual years in the 1950ies to 1970ies with high peaks in ^{14}C production caused by nuclear bomb testing (Naegler and Levin 2006) (figure S1C). Potential impacts of ^{14}C production from the nuclear industry (Graven and Gruber 2011, Graven 2015) are tested with sensitivity runs (see supplementary material for details on ^{14}C production rate). All simulations are started in year 10 000 BP to allow the ^{14}C cycle to adjust to variable production rates.

For model evaluation (supplementary material) the simulated time series of atmospheric CO_2, $\delta^{13}C$ and $\Delta^{14}C$ are then compared with historical data from both ice cores and instrumental records (figure S2), but also with the proposed atmospheric CO_2 concentrations of the RCP emission scenarios (Moss *et al* 2010, Meinshausen *et al* 2011) that should be taken as radiative forcing time series in the CMIP5 model intercomparison project.

Additionally I investigate three different methods of CDR, (a) bioenergy with capture and storage (BECCS), (b) direct air capture (DAC), and (c) ocean alkalinization or enhanced weathering (EW), which all interact with the carbon cycle in completely different ways. I prescribe the strength of these three methods in order to linearly reduce net carbon emissions from 2021 onward until an annual net removal of 5 Pg C yr^{-1} is achieved in the year 2050, and maintained thereafter. Alternatively, after year 2070 the 5 Pg C yr^{-1} net CO_2 removal would cease (scenarios BECCSs, DACs and EWs), and the simulations would continue. In DAC carbon is extracted from the atmospheric pool and assumed to be permanently stored in some geological reservoir without any further exchange with the atmosphere-ocean-terrestrial biosphere subsystem of the carbon cycle. The storage is similar in BECCS, but the extraction of carbon is based in biologically produced organic carbon, implying that isotopic fractionation during photosynthesis took place first, having a net effect on the carbon isotopes, and making BECCS similar to a land use change scenario with negative emissions. In EW an enhanced weathering or ocean alkalinization flux is calculated that approximates the desired CO_2 removal: 1 mol of desired CO_2 removal triggers the input of 1 mol of bicarbonate ion (HCO_3^-) into the surface ocean, which would be the product of any man-made EW by enhanced silicate weathering that changes both the carbon content and the alkalinity in the ocean and ultimately the CO_2 uptake capacity of the world oceans. In practical terms the molar input of HCO_3^- can be related to the necessary amount of silicate rocks that needs to be dissolved by the relevant net chemical dissolution equations, e.g. 1 g of olivine (Mg_2SiO_4 with about 140 g mol^{-1}) would lead to a theoretical input of $1/140 \times 4 = 0.03$ mol of HCO_3^- (for details see Köhler *et al* 2010, Griffioen 2016). Any second order effects of enhanced silicate rock weathering that might occur due to changes in the biological pump (Köhler *et al* 2013, Hauck *et al* 2016) are ignored here.

The isotopic signature of fluxes related to BECCS, DAC and EW are consistently calculated within the model: both the CO_2 extracted within BECCS and DAC and the influx of HCO_3^- into the surface ocean during EW contain the $\delta^{13}C$ and $\Delta^{14}C$ signatures of the atmospheric reservoir during the relevant time step (additionally within BECCS isotopic fractionation by −19‰ due to photosynthesis is considered). The differences in the isotopic signatures of the RCP and CDR fluxes are the reason why both the emission and the CO_2 removal fluxes need to be prescribed individually, and not only as one net flux. The size of BECCS as assumed in RCP2.6, RCP4.5, and RCP6.0 in the 21st century is assumed to stay constant on its 2100 level thereafter (figure 1(B)).

3. Results and discussions

My discussion of carbon cycle results is focused on the RCP8.5 emission scenario and subsequent CDR approaches diverging from it. However, the results for the other scenarios (RCP2.6, RCP4.5, RCP6.0) are included in the figures and the effects on the carbon isotopes in them is contained in my analysis of the combined Suess effects.

3.1. Carbon cycle dynamics

In the RCP8.5 emission scenario mitigation efforts start late leading to anthropogenic emission rates of up to nearly 30 Pg C yr^{-1} around year 2100 with an assumed linear reduction between 2150 and 2200 to a constant emission rate of 1.5 Pg C yr^{-1} until year

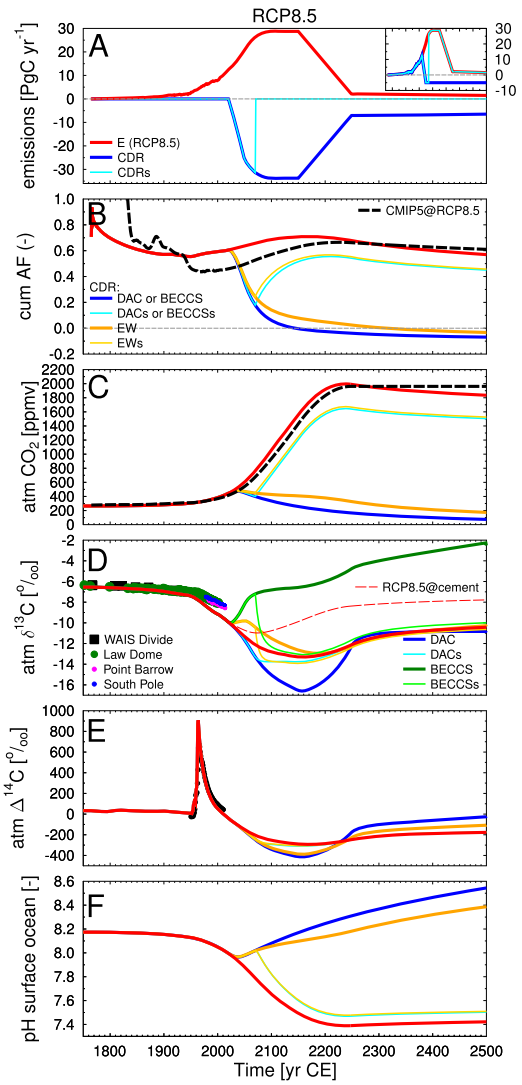

Figure 2. Carbon cycle simulation results from pre-industrial times until year 2500. Results are based on RCP8.5 emission scenario (Meinshausen *et al* 2011) including carbon dioxide reduction (CDR) via bioenergy and carbon capture and storage (BECCS), direct direct air capture (DAC) and enhanced weathering (EW). BECCS and DAC differ only in $\delta^{13}C$, changes in $\Delta^{14}C$ are on the order of a few permil only and negligible. (A) Emission rate E of RCP8.5 in the extended scenario until 2500 and the negative emissions of CDR approaches. Small inlet sketches the net emissions (E–CDR in PgC yr^{-1}). (B) Cumulative airborne fraction (AF): $\Delta A/\sum E$ with ΔA change in atmospheric C content and $\sum E$ the cumulative sum of emissions. (C) Simulated atmospheric CO_2, black broken line is the past reconstruction of CO_2 (instrumental at Mauna Loa) (Keeling and Whorf 2005) and Law Dome ice core (Rubino *et al* 2013) or the mean of projected future concentrations within CMIP5 for RCP8.5 (Meinshausen *et al* 2011); (D) Simulated atmospheric $\delta^{13}C$ and reconstructions (instrumental: Point Barrow, South Pole, Keeling *et al* 2001, ice cores: Law Dome and WAIS Divide, Rubino *et al* 2013, Bauska *et al* 2015). RCP8.5@cement is a sensitivity study in which the source of the fossil fuel emission is slowly shifting from today 6% to 100% cement in year 2250. Cement has a $\delta^{13}C$ signature of 0‰. (E) Simulated atmospheric $\Delta^{14}C$ including in black the reconstructed radiocarbon bomb peak (Hua *et al* 2013). (F) Simulated mean *p*H of the surface ocean.

2500. (figure 2(A)). These emissions would result in a rise in atmospheric CO_2 concentration from present day 400 ppmv to ~2000 ppmv after year 2200 in both the CMIP5 scenarios (Meinshausen *et al* 2011) and my carbon cycle simulations (figure 2(C)). The global warming and ocean acidification connected with such a rise in the most important anthropogenic greenhouse gas would be severe leading in my simulations to a temperature rise of 5–6 K (figure S3) and a drop in mean surface ocean pH by 0.8 units (from 8.2 to 7.4) (figure 2(F) inlet).

Within the hypothetical CDR scenarios investigated here, net emissions are reduced even faster than in the other RCP emission scenarios assuming negative net emissions from year 2040 onward (figure 2(A)) and therefore broaden the range of possible future scenarios. The carbon extraction achieved in these CDR simulations might be unrealistically high, however, my interest here lies in showing potential maximum impacts on the carbon isotopes and not to investigate the most plausible scenario.

The cumulative airborne fraction (AF) of the anthropogenic emissions E (Pg C yr^{-1}), here defined as the ratio in the difference in atmospheric carbon pool (with respect to the pre-industrial values in year 1765) over the cumulative sum of E, stays in my simulations around 0.6 (figure 2(B)). Cumulative AF calculated from emission driven CMIP5 data are before year 1830 larger than 1, probably due to carbon cycle internal variability not driven by the yet small anthropogenic emissions. In the 21st and 22nd centuries they are slightly smaller than in my simulations. This difference is explained with the passive (=constant) terrestrial carbon pools in my simulations which neglects the terrestrial carbon sink found in the historical data (Le Quéré *et al* 2015). I refrain from showing results with active (=variable) terrestrial carbon cycle, since for atmospheric CO_2 concentrations well above 500 ppmv, the CO_2 fertilization implemented in my simple model is much too large, when compared with CMIP5 models, leading, due to the massive buildup of terrestrial carbon, to unrealistically low atmospheric CO_2 concentration (Köhler *et al* 2015). I here restrict simulation results to those obtained with an atmosphere-ocean only setup of the the carbon cycle, which on the long run agree in the atmospheric carbon pools with those of the CMIP5 results, although the still existing uncertainty in the land carbon cycle, partly due to an overestimation of the CO_2 fertilization (Smith *et al* 2016a), or due to uncertainties in the nitrogen cycle (Meyerholt *et al* 2016) might indicate that CMIP5 results are also not perfect. On the long run the cumulative AF and atmospheric CO_2 of my simulations converge with those based on CMIP5, indicating a small long-term influence of the terrestrial carbon sink in models contributing to CMIP5 (figures 1(C) and 2(B)). Simulations including terrestrial carbon storage changes would result in smaller simulated atmospheric CO_2, smaller AFs, and less depleted atmospheric $\delta^{13}C$. Therefore, the historical ^{13}C Suess effect is better matched by using an active terrestrial carbon cycle (figure S2B), while the effect on the historical ^{14}C Suess effect reduces the offset

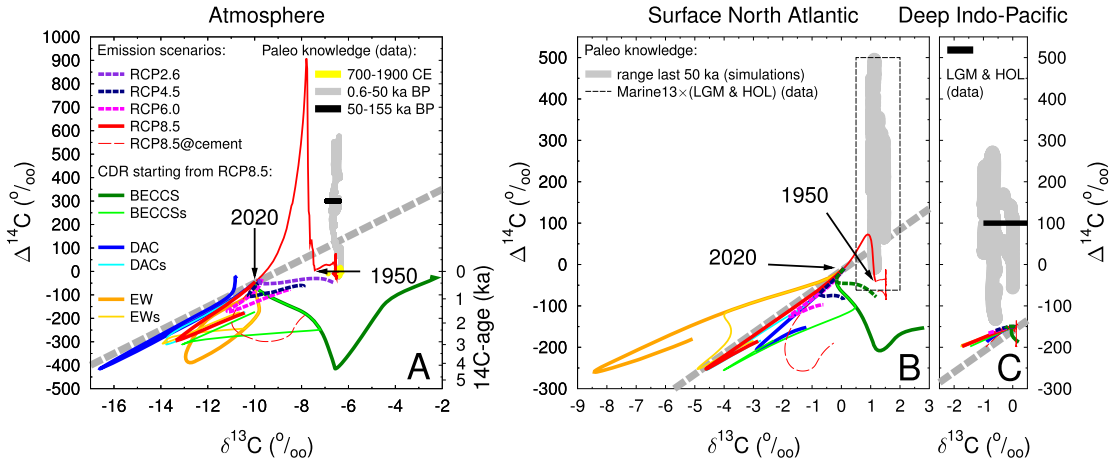

Figure 3. Analysis of the combined Suess effects on both ^{14}C and ^{13}C. Scatter plot of simulated $\Delta^{14}C$ versus $\delta^{13}C$ (A) atmosphere, (B), (C): end-members within the ocean (surface North Atlantic, deep Indo-Pacific) showing the historical and future Suess effects and the influence of bomb-^{14}C, future CO_2 emissions and carbon dioxide reduction (CDR) approaches (BECCS, DAC, EW) on both variables. Also included in dotted lines are results for RCP2.6, RCP4.5 and RCP6.0, which all contain a prescribed contribution of BECCS (see figure 1 for details). The right *y*-axis in panel (A) also provides, similarly as before in Graven 2015, a conventional calculated ^{14}C-age $= 8033 \times \ln(\Delta^{14}C/1000 + 1)$ for all $\Delta^{14}C$ values below zero (1 ka = 1000 years). For comparison, also the available paleo knowledge is added: (A) Atmospheric $\delta^{13}C$ from ice cores (700–1900 CE: WAIS Divide ice core, Bauska *et al* 2015; further back in time: spline through ice core compilation, Eggleston *et al* 2016) and $\Delta^{14}C$ from IntCal13 (Reimer *et al* 2013), for 50–155 ka BP plotted with fixed $\Delta^{14}C = 300‰$; In the ocean I show the data range obtained from sediment cores in $\delta^{13}C$ (Peterson *et al* 2014) obtained for the Last Glacial Maximum (LGM) and the late Holocene (HOL) for (B) the range of surface ocean $\Delta^{14}C$ contained in Marine13 (Reimer *et al* 2013) or (C) for a fixed value of $\Delta^{14}C = 100‰$. Additionally, the range in both isotopes in previously published (imperfect) simulations using the BICYCLE model covering the last 50 000 year (50 ka) is shown (upper limit of scenario S3x (^{14}C production rate based on ^{10}Be) and lower limit of scenario S4x (^{14}C production rate based on reconstructions of the geomagnetic field strength GLOPIS-75) as used before in Köhler *et al* 2006). The gray broken line in all subplots crosses values for year 2020 with a slope $m = 50$ (see text for further explanation).

between model and data, but has negligible impact on the ^{14}C dynamic (figure S2C).

All CDR methods have a permanent impact on atmospheric CO_2 concentrations and on surface ocean pH (figures 2(C), (F)). Even in the scenarios BECCSs, DACs and EWs, in which CDR is stopped after some decades (here in year 2070) the simulated CO_2 concentrations (and surface ocean pH) do not reach the values obtained without CDR. The assumed CDR scenarios would eventually lead to a cumulative AF of zero, implying that an amount of CO_2 identical to the sum of all anthropogenic CO_2 emissions has been extracted from the carbon cycle again and atmospheric CO_2 concentration starts to fall below pre-industrial values.

3.2. Carbon isotopes: the ^{14}C and ^{13}C Suess effects

The carbon isotopes of atmospheric CO_2 are both depleted by the massive injection of anthropogenic emissions, since fossil fuels are ^{14}C-free and contain with about −24 to −29‰ a $\delta^{13}C$ signature (Andres *et al* 2000, 2015) that is 19‰ lighter than the $\delta^{13}C$ signature of the atmospheric CO_2 itself (figure S1B). Additionally, the radiocarbon cycle is penetrated by the bomb-^{14}C emissions in the second half of the last century (Naegler and Levin 2006) leading around 1965 to atmospheric $\Delta^{14}C$ values of up to $+700 \pm 200‰$ in the data (Hua *et al* 2013) and of +900‰ in my simulations (figure 2(E)) (see supplementary material for further details).

Atmospheric $\Delta^{14}C$ then drops around 2150 to −300‰ in RCP8.5 and to −415‰ in all CDR approaches. This most depleted $\Delta^{14}C$ signature of −415‰ is identical to that of a 4300 year old carbon sample (figure 3(A)). Depending on the assumed CDR method $\delta^{13}C$ of atmospheric CO_2 drops at the same time to values of (RCP8.5) −13.3‰, (EW) −12.6‰, or (DAC) −16.6‰ (figure 2(D)). For BECCS $\delta^{13}C$ of atmospheric CO_2 returns to its pre-industrial value of −6.5‰ in year 2150 and rises thereafter to values up to −2‰. Here, the difference of how the CDR methods modify the carbon cycle has a significant impact on the resulting atmospheric $\delta^{13}C$ signature: BECCS operates as negative land use change, therefore reversing the ^{13}C Suess effect. In scenario EW alkalinity is added to the ocean. The isotopic fractionation within the dissolved inorganic carbon (DIC) in the ocean and therefore of the ocean-atmosphere gas exchange depends directly on the concentration of HCO_3^- and CO_3^{2-}, two of the chemical species of DIC. However, the concentrations of these species change with a rise in alkalinity to allow a larger oceanic CO_2 storage. Therefore, the isotopic fractionation during gas exchange indirectly depends on the surface ocean alkalinity (Zeebe and Wolf-Gladrow 2001) and is in detail implemented in BICYCLE similarly as in other models (Ridgwell 2001).

When $\Delta^{14}C$ and $\delta^{13}C$ are plotted against each other it clearly becomes evident that the Suess effects on both isotopes will in the future bring the isotopic

carbon cycle into a regime in which it has not been during at least the last 50 000 years. The historical Suess effect before 1950 (−0.7‰ in $\delta^{13}C$ and −20‰ in $\Delta^{14}C$) already shifted the atmospheric variables away from its natural state (figure 3(A)). The atmospheric $\Delta^{14}C$ simulated in response to the bomb-^{14}C injection led to 0 to +900‰, slightly larger than the range of −25-to- +575‰ that has been reconstructed for the pre-industrial 50 000 years from various archives (Köhler *et al* 2006, Reimer *et al* 2013). Already the historical emissions from 1950 onward including the foreseeable emissions until 2020 shift the atmospheric $\delta^{13}C$ by another −2‰. In most scenarios a further depletion in both carbon isotopes takes place in the near future. At the extreme, values of $\Delta^{14}C = -415‰$ and $\delta^{13}C = -16.6‰$ are reached in the atmospheric carbon reservoir. The exceptions to this rule are scenarios in which BECCS plays a dominant role, also implying that RCP2.6 has a different dynamic in the carbon isotopes than the other RCP scenarios. EW would first lead to a small rise in $\delta^{13}C$ but on the long run also to a depletion. In BECCS the simulated $\delta^{13}C$ on the long run is higher than what is known from the paleo record. Most scenarios might, after having a maximum depletion in the isotopic phase space, return to less extreme anomalies in both isotopes, only RCP2.6 returns in the $\Delta^{14}C$–$\delta^{13}C$-scatter plot back to conditions seen in pre-industrial times or found in the paleo simulations or reconstructions.

To analyze how the carbon isotopes in the ocean might change due to the Suess effects I focus on the two end-member in the oceanic carbon cycle: (a) North Atlantic surface waters, where North Atlantic Deep Water formation occurs and a dominant part of deep ocean water masses have last contact with the atmosphere and (b) the deep Indo-Pacific, in which the oldest, most $\Delta^{14}C$-depleted water masses are found. A similar pattern as found in the atmosphere emerges in the North Atlantic surface waters, although with smaller amplitude (figure 3(B)): the bomb-^{14}C spike is found with slightly more than +100‰, the ^{13}C Suess effect leads until 2020 to a reduction in $\delta^{13}C$ by nearly −1.5‰, and all scenarios but RCP2.6 enter uncharted waters in the $\Delta^{14}C$–$\delta^{13}C$ phase space. Clearly seen is also that the rising ocean alkalinity in the EW CDR method leads to a more depleted surface ocean $\delta^{13}C$, explaining the lower isotopic fractionation (less depletion) in the atmospheric $\delta^{13}C$ record and the special dynamics for BECCS leading to $\delta^{13}C$ of nearly +3‰. An overlap of the historical and future simulations with the data range spanned by paleo data (Reimer *et al* 2013, Peterson *et al* 2014) and paleo simulations (Köhler *et al* 2006) covering the last 50 000 years is only obtained for the bomb-^{14}C spike. Also note, that these paleo simulations, performed with a previous version of the same model, were imperfect, since they were not able to explain the full decline in atmospheric $\Delta^{14}C$ found in the paleo reconstructions (Reimer *et al* 2013).

The simulated changes in the deep Indo-Pacific during the next five centuries are much smaller than for the surface ocean (figure 3(C)). Until 2020 the Suess effects or even the ^{14}C-bomb spike are not detectable in this reservoir, however the effect of further anthropogenic emissions will over the course of the simulations found its way to this most remote ocean reservoir and both Suess effects will then be visible there. The simulated future trends in the deep Indo-Pacific $\delta^{13}C$ have some overlap with the range of reconstructed $\delta^{13}C$, however, the knowledge on deep ocean $\Delta^{14}C$ is still limited. While my previous (imperfect) simulations suggest that deep Indo-Pacific $\Delta^{14}C$ was always higher than −150‰ throughout the last 50,000 years, the limited available deep ocean $\Delta^{14}C$ reconstructions show a different picture (Ronge *et al* 2016): $\Delta^{14}C$-values as low as −200‰ are found in waters above 2000 m and below 4300 m water depth in the South Pacific with some water masses in between (and in intermediate depths of ∼600 m around the Galapagos Islands (Stott *et al* 2009) having during the last 25 000 years a $\Delta^{14}C$ signature as low as −600‰. This would imply that for most of the RCP emission scenarios the deep Pacific data in the $\Delta^{14}C$–$\delta^{13}C$ phase space might already have been obtained in some form during glacial conditions in the past. These most recent deep Pacific data with low $\Delta^{14}C$ signature (Ronge *et al* 2016) are not yet completely understood. It is not yet clear how wide-spread this water mass is and the explaining hypothesis put forward so far suggests the release of ^{14}C-free CO_2 from hydrothermal activities along mid-ocean ridges during sea-level low stand in glacial times. This would imply that the deep glacial ocean would contain, in addition to the fossil fuel emissions into the atmosphere, another source of ^{14}C-free carbon. The interpretation of deep ocean carbon isotopic signatures might therefore be not yet straightforward.

Simulation results for other surface ocean reservoirs are qualitatively similar to the North Atlantic surface end member discussed in detail above (figure S4), allowing in surface reservoirs to use the ^{13}C Suess effect to distinguish past from future carbon fluxes. Interestingly, the largest oceanic anomalies in $\delta^{13}C$ are obtained in the surface equatorial Atlantic Ocean (figure S4B) with $\delta^{13}C$ falling down to −13‰ for EW scenarios, probably caused by the way the EW fluxes are prescribed. These fluxes enter the surface ocean only in the equatorial regions, with 50% each routed in the Atlantic and Indo-Pacific. Combined with the smaller size of the Atlantic basin, the effect of EW on the local carbon cycle is more pronounced in the Atlantic than in the Indo-Pacific. Since the prescribed water mass fluxes to the surface North Pacific area are all sourced in deep ocean regions, $\delta^{13}C$ in this area follows in the EW scenarios the dynamics seen in the atmosphere (less depleted than in RCP8.5, figure S4F). Carbon isotopic dynamics in the deep ocean of the

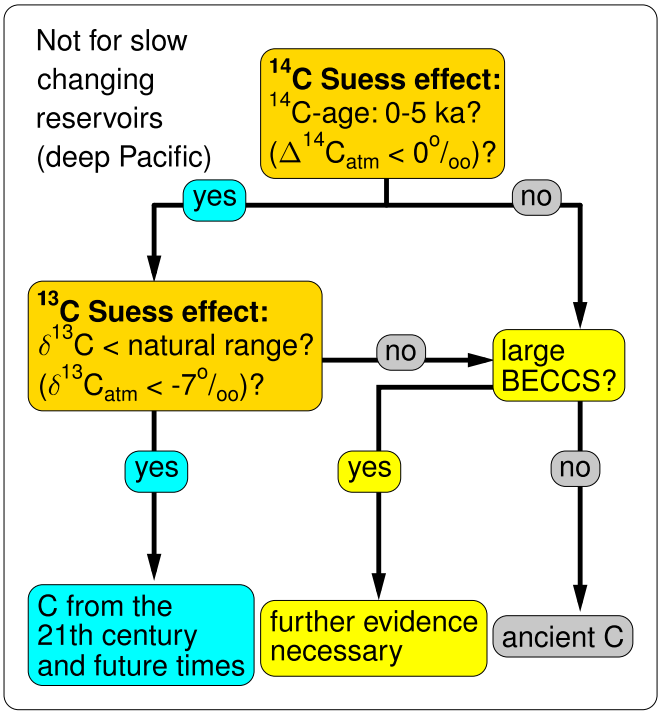

Figure 4. Decision tree how to distinguish ancient carbon from carbon which requires an age marker from future times. The combination of radiocarbon dating and how $\delta^{13}C$ needs to leave its natural range due to the combined ^{14}C and ^{13}C Suess effects with examples for the atmospheric reservoir are given. For cases in which CDR by a large contribution of BECCS is realized (e.g. as in RCP2.6) the carbon isotopic signatures might return back to pre-industrial values. For these cases further not yet identified evidence is necessary to distinguish ancient from future carbon. For slow changing reservoirs, e.g. the deep Pacific, changes for the future overlap with past data ranges, so a clear identification of ancient versus future carbon is not possible.

Atlantic (figure S4C) and to some extend in the Southern Ocean (figure S4E) depart from known data ranges in the past. My approach to disentangle past from future carbon cycle changes therefore seemed also to be applicable to data from these deep ocean reservoirs. Further regional details are better obtained with spatially higher resolved models.

Fossil fuel fluxes contain also emissions from industrial processes, namely cement production. The $\delta^{13}C$ signature of fossil fuels therefore depends on the source mix and ranges from 0‰ (cement production) to −44‰ (natural gas) (Andres *et al* 2000). About 6% of the CO_2 emissions summarized as fossil fuels in year 2014 have been from cement production (Le Quéré *et al* 2015). In my standard scenarios I assume that the source mix (and therefore the $\delta^{13}C$ signature of fossil fuels) remains the same from year 2011 onward. In one scenario (RCP8.5@cement) I test the effect when cement production would slowly become the one and only source of the fossil fuel emissions in year 2250 (evolution of $\delta^{13}C$ of fossil fuels shown in figure S1B). Simulated $\delta^{13}C$ values would then be less depleted than in our standard simulations (figure 2(D)), but isotopic values would still be outside of their ranges known from the past (figure 3), and the overall conclusion would therefore not be affected by such a rise in the relative importance of cement in the source mix of future fossil fuel emissions.

4. Conclusions

When considering not only the ^{14}C Suess effect but also the ^{13}C Suess effect the future changes in the carbon isotopes in the atmosphere and the neighboring reservoirs (surface ocean, to some extend relatively fast ventilated water masses of the deep ocean, but also terrestrial biosphere) follow a distinct pattern that makes them distinguishable from variability in the past. This study is after the initial modeling study (Keeling 1979) one of a few approaches (e.g. Jahn *et al* 2015) in which both Suess effects are considered together. Simulation studies typically focus on either the ^{14}C Suess effect (Caldeira *et al* 1998, Graven 2015) or ^{13}C Suess effect (Gruber *et al* 1999, Tagliabue and Bopp 2008, Schmittner *et al* 2013). Changes in the carbon isotopic signature can be approximated from theory by considering that the injection of ^{14}C-free fossil fuels with a $\delta^{13}C$ signature of −28‰ leads to a carbon influx that differs from the present day atmosphere by $\Delta(\Delta^{14}C) \approx -1000‰$ and $\Delta(\delta^{13}C) \approx -20‰$. These differences are equivalent to a linear change with a slope $m = -1000‰/-20‰ = 50$ in the $\Delta^{14}C$–$\delta^{13}C$ phase space as indicated by the broken lines in figures 3 and S4. The realized simulations that do not contain CDR due to BECCS or EW, nearly meet this theoretical expectation.

I therefore propose that measuring ^{13}C in parallel to ^{14}C measurements will enable researchers to distinguish

the future from the past in radiocarbon. This approach should be applicable for carbon reservoirs that are in reasonable fast exchange with the atmosphere to allow any Suess effect to be visible in the data sets. For data from deep ocean sites, especially from the Indo-Pacific, the observed future variability in the carbon isotopes might be too small to identify a clear excursion from past data ranges. If a ^{14}C-age falls within the range of 0 to 5000 years (corresponding to Δ^{14}C in the atmosphere of approximately 0 to −450‰) a cross-check on the ^{13}C Suess effect is necessary (figure 4). Here, isotopic fractionation during photosynthesis needs to be taken into account, if the relevant probe was derived for organic carbon. If the carbon cycle has been heavily perturbed by both Suess effects, the probe has its origin (age) within this or future centuries. If no ^{13}C Suess effect can be detected then the relevant carbon is of ancient origin, e.g. it had its last contact with the atmosphere in the past before fossil fuels perturbed the carbon cycle. For the exception that a large contribution of CDR is obtained via BECCS further evidences might be necessary since the carbon cycle might then not leave the Δ^{14}C–δ^{13}C-space known from historical and paleo reconstructions. I am aware that this isotopic fractionation during photosynthesis depends on various factors and might itself lead to a wide range of δ^{13}C within any organic material (Lloyd and Farquhar 1994), even without any perturbations of the ^{13}C Suess effect. Therefore, expert knowledge on the expected natural range of δ^{13}C within the any organic material is certainly necessary to make this final conclusion.

Earth system models contributing to CMIP5 including an active terrestrial biosphere might reduce uncertainties in the simulated future carbon cycle dynamics. The general pattern found here with a simplified carbon cycle model that the ^{13}C Suess effect might be used to distinguish between past and future carbon sources, however, is robust and should not change if investigated with more complex models.

Acknowledgments

The design of the CDR scenarios was motivated by initially proposed scenarios within the CDR-MIP project. Thanks to the RCP core group and Heather Graven for providing data on the amplitude of BECCS within the RCP scenarios. I thank Dieter Wolf-Gladrow and Gregor Knorr for helpful comments. Simulation results are available from the data base PANGAEA (doi: 10.1594/PANGAEA.868739).

References

Andres R, Boden T and Marland G 2015 *Annual Fossil-Fuel CO_2 Emissions: Global Stable Carbon Isotopic Signature* Carbon Dioxide Information Analysis Center, Oak Ridge National Laboratory, U.S. Department of Energy Oak Ridge, Tenn, USA (http://cdiac.ornl.gov/ndps/db1013_v2015.html)

Andres R, Marland G, Boden T and Bischof S 2000 Carbon dioxide emissions from fossil fuel consumption and cement manufacture, 1751–1991, and an estimate of their isotopic composition and latitudinal distribution *The Carbon Cycle* ed T Wigley and D Schimel (Cambridge: Cambridge University Press) pp 53–62

Bauska T K, Joos F, Mix A C, Roth R, Ahn J and Brook E J 2015 Links between atmospheric carbon dioxide, the land carbon reservoir and climate over the past millennium *Nat. Geosci.* **8** 383–7

Caldeira K, Rau G H and Duffy P B 1998 Predicted net efflux of radiocarbon from the ocean and increase in atmospheric radiocarbon content *Geophys. Res. Lett.* **25** 3811–4

Cao L and Caldeira K 2010 Atmospheric carbon dioxide removal: long-term consequences and commitment *Environ. Res. Lett.* **5** 024011

Eggleston S, Schmitt J, Bereiter B, Schneider R and Fischer H 2016 Evolution of the stable carbon isotope composition of atmospheric CO_2 over the last glacial cycle *Paleoceanography* **31** 434–52

Graven H D 2015 Impact of fossil fuel emissions on atmospheric radiocarbon and various applications of radiocarbon over this century *Proc. Natl Acad. Sci.* **112** 9542–5

Graven H D and Gruber N 2011 Continental-scale enrichment of atmospheric $^{14}CO_2$ from the nuclear power industry: potential impact on the estimation of fossil fuel-derived CO_2 *Atmos. Chem. Phys.* **11** 12339–49

Griffioen J 2016 Enhanced weathering of olivine in seawater: the efficiency as revealed by thermodynamic scenario analysis *Sci. Total Environ.* in press (doi:10.1016/j.scitotenv.2016.09.008)

Gruber N, Keeling C D, Bacastow R B, Guenther P R, Luecker T J, Wahlen M, Meijer H A J, Mook W G and Stocker T F 1999 Spatiotemporal patterns of carbon-13 in the global surface oceans and the oceanic Suess effect *Glob. Biogeochem. Cycles* **13** 307–35

Hauck J, Köhler P, Wolf-Gladrow D A and Völker C 2016 Iron fertilisation and century-scale effects of open ocean dissolution of olivine in a simulated CO_2 removal experiment *Environ. Res. Lett.* **11** 024007

Houghton R A 2003 Revised estimates of the annual net flux of carbon to the atmosphere from changes in land use and land management 1850-2000 *Tellus* **55B** 378–90

Hua Q, Barbetti M and Rakowski A Z 2013 Atmospheric radiocarbon for the period 1950–2010 *Radiocarbon* **55** 2059–72

Iyer G C *et al* 2015 The contribution of Paris to limit global warming to 2 °C *Environ. Res. Lett.* **10** 125002

Jahn A, Lindsay K, Giraud X, Gruber N, Otto-Bliesner B L, Liu Z and Brady E C 2015 Carbon isotopes in the ocean model of the Community Earth System Model (CESM1) *Geosci. Model Dev.* **8** 2419–34

Keeling C D 1979 The Suess effect: ^{13}Carbon-^{14}Carbon interrelations *Environ. Int.* **2** 229–300

Keeling C D, Bollenbacher A F and Whorf T P 2001 Exchanges of atmospheric CO_2 and $^{13}CO_2$ with the terrestrial biosphere and oceans from 1978 to 2000 *I. Global aspects, SIO Reference Series, No. 01-06* Scripps Institution of Oceanography, San Diego 88 pp

Keeling C D and Whorf T P 2005 Atmospheric CO_2 records from sites in the SIO air sampling network *Trends: A Compendium of Data on Global Change* Carbon Dioxide Information Analysis Center, Oak Ridge National Laboratory, U.S. Department of Energy, Oak Ridge, Tenn, USA

Knutti R, Rogelj J, Sedlacek J and Fischer E M 2016 A scientific critique of the two-degree climate change target *Nat. Geosci.* **9** 13–8

Köhler P, Abrams J F, Völker C, Hauck J and Wolf-Gladrow D A 2013 Geoengineering impact of open ocean dissolution of olivine on atmospheric CO_2, surface ocean pH and marine biology *Environ. Res. Lett.* **8** 014009

Köhler P, Fischer H, Munhoven G and Zeebe R E 2005 Quantitative interpretation of atmospheric carbon records over the last glacial termination *Glob. Biogeochem. Cycles* **19** GB4020

Köhler P, Hartmann J and Wolf-Gladrow D A 2010 Geoengineering potential of artificially enhanced silicate weathering of olivine *Proc. Natl Acad. Sci.* **107** 20228–33

Köhler P, Hauck J, Völker C and Wolf-Gladrow D 2015 Interactive comment on a simple model of the anthropogenically forced CO_2 cycle *Earth Syst. Dyn. Discuss.* **6** C813 (www.earth-syst-dynam-discuss.net/6/C813/2015/esdd-6-C813-2015.pdf)

Köhler P, Muscheler R and Fischer H 2006 A model-based interpretation of low frequency changes in the carbon cycle during the last 120,000 years and its implications for the reconstruction of atmospheric $\Delta^{14}C$ *Geochem. Geophys. Geosyst.* **7** Q11N06

Le Quéré C C *et al* 2015 Global carbon budget 2015 *Earth Syst. Sci. Data* **7** 349–96

Lloyd J and Farquhar G D 1994 ^{13}C discrimination during CO_2 assimilation by the terrestrial biosphere *Oecologia* **99** 201–15

Meinshausen M *et al* 2011 The RCP greenhouse gas concentrations and their extensions from 1765 to 2300 *Clim. Change* **109** 213–41

Meyerholt J, Zaehle S and Smith M J 2016 Variability of projected terrestrial biosphere responses to elevated levels of atmospheric CO_2 due to uncertainty in biological nitrogen fixation *Biogeosciences* **13** 1491–518

Moss R H *et al* 2010 The next generation of scenarios for climate change research and assessment *Nature* **463** 747–56

Naegler T and Levin I 2006 Closing the global radiocarbon budget 1945–2005 *J. Geophys. Res.* **111** D12311

Peterson C D, Lisiecki L E and Stern J V 2014 Deglacial whole-ocean $\delta^{13}C$ change estimated from 480 benthic foraminiferal records *Paleoceanography* **29** 549–63

Reimer P J *et al* 2013 IntCal13 and Marine13 radiocarbon age calibration curves 0–50,000 years cal BP *Radiocarbon* **55** 1869–87

Ridgwell A J 2001 Glacial-interglacial perturbations in the global carbon cycle *PhD Thesis* University of East Anglia Norwich, UK

Rogelj J, McCollum D L, O'Neill B C and Riahi K 2013 2020 emissions levels required to limit warming to below 2°C *Nat. Clim. Change* **3** 405–12

Rogelj J, Schaeffer M, Meinshausen M, Knutti R, Alcamo J, Riahi K and Hare W 2015 Zero emission targets as long-term global goals for climate protection *Environ. Res. Lett.* **10** 105007

Ronge T, Tiedemann R, Lamy F, Köhler P, Alloway B V, Pol-Holz R, Pahnke K, Southon J and Wacker L 2016 Radiocarbon constraints on the extent and evolution of the Pacific glacial carbon pool *Nat. Commun.* **7** 11487

Roth R and Joos F 2013 A reconstruction of radiocarbon production and total solar irradiance from the Holocene ^{14}C and CO_2 records: implications of data and model uncertainties *Clim. Past* **9** 1879–909

Rubino M *et al* 2013 A revised 1000-year atmospheric $\delta^{13}C$-CO_2 record from Law Dome and South Pole, Antarctica *J. Geophys. Res.: Atmos.* **118** 8482–99

Schmittner A, Gruber N, Mix A C, Key R M, Tagliabue A and Westberry T K 2013 Biology and air-sea gas exchange controls on the distribution of carbon isotope ratios ($\delta^{13}C$) in the ocean *Biogeosciences* **10** 5793–816

Smith K W, Reed S C, Cleveland C C, Ballantyne A P, Anderegg W R L, Wieder W R, Liu Y Y and Running S W 2016a Large divergence of satellite and Earth system model estimates of global terrestrial CO_2 fertilization *Nat. Clim. Change* **6** 306–10

Smith P *et al* 2016b Biophysical and economic limits to negative CO_2 emissions *Nat. Clim. Change* **6** 42–50

Stott L, Southon J, Timmermann A and Koutavas A 2009 Radiocarbon age anomaly at intermediate water depth in the Pacific Ocean during the last deglaciation *Paleoceanography* **24** A2223

Stuiver M and Quay P D 1981 Atmospheric ^{14}C changes resulting from fossil fuel CO_2 release and cosmic ray flux variability *Earth Planet. Sci. Lett.* **53** 349–62

Suess H E 1955 Radiocarbon concentration in modern wood *Science* **122** 415–7

Swart P K, Greer L, Rosenheim B E, Moses C S, Waite A J, Winter A, Dodge R E and Helmle K 2010 The ^{13}C Suess effect in scleractinian corals mirror changes in the anthropogenic CO_2 inventory of the surface oceans *Geophys. Res. Lett.* **37** L05604

Tagliabue A and Bopp L 2008 Towards understanding global variability in ocean carbon-13 *Glob. Biogeochem. Cycles* **22** GB1025

van Vuuren D P *et al* 2011 The representative concentration pathways: an overview *Clim. Change* **109** 5–31

Zeebe R E and Wolf-Gladrow D A 2001 *CO_2 in Seawater: Equilibrium, Kinetics, Isotopes* (*Elsevier Oceanography Book Series* vol 65) (Amsterdam: Elsevier)